METABOLIC INTERACTIONS AND COMMUNITIES: CO-METABOLISM OR NO-METABOLISM

October 29, 2019

Will Sharpless
UC Berkeley
C112L Microbiology Lab

0.1 Abstract

Microbial communities dominate the environment and consist of the most untamed biological dynamics yet to be understood and engineered. In the work, we sought to investigate the potential of a shared metabolite interaction to establish a synthetic two-member community of *Escheria coli* auxotrophs Δ*melA* and Δ*galK*. We proved that we successfully established a community through growth cultures with dialysis barriers and high-throughput Biolog fitness assays. The compromising densities of each member in the combined cultures demonstrated the finite nature of ecological communities and how seemingly benign interactions can supplant negative feedback in a closed system. Our work serves a model for understanding how communal interactions might arise and develop in settings with physical barriers.

0.2 Introduction

Metabolic interactions define microbial community structure [1, 2]. While direct contact and gene flow may be impeded by physical barriers [3, 4], a small molecule (or congruently its absence) serves as a network between organisms separated by miles [5]. Magnified by the size of the population, the interactions amount to governing forces in a microbial community that stabilize populations and allow them to occlude foreign invasion [6]. Moreover, many metabolic interactions have proven ample conduits for controlling microbiome outputs in bioremediation [7], agriculture [8] and and human health [9,10,11]. By studying interactions and their influence on the overall community, we may develop new methods for controlling microbiomes as well as reveal their evolutionary origins.

In the work, we sought to constitute a synthetic, two-member community in order to elucidate how intraspecies, metabolic connections might influence the health of species independently. We manifested the community through interdependecies of *Escheria coli* auxotrophs, ΔmelA and ΔgalK [12]. *E. coli* was an optimal vehicle for our study because its metabolism is well characterized [12] and allowed us to predict our results with precision as well as compare our results with a large body of work [13]. The chosen mutants are independently impaired on specific carbohydrates but together complete a lop-sided catabolic pathway (Figure 1). α-Galactosidase (melA) is the initial enzyme in the degradation of melibiose, and catalyzes the hydrolysis of melibiose into D-Galactose and D-Glucose [14]; the melA knockout is unable to utilize melibiose as a sole carbon

source [15]. Galactose Kinase (galK) commits galactose to the Leloir pathway by phosphorylating α-D-Galactose at the 1' position [16]; galK is essential for the degradation of galactose [16]. Both pathways flow into glycolytic pathways toward the TCA cycle.

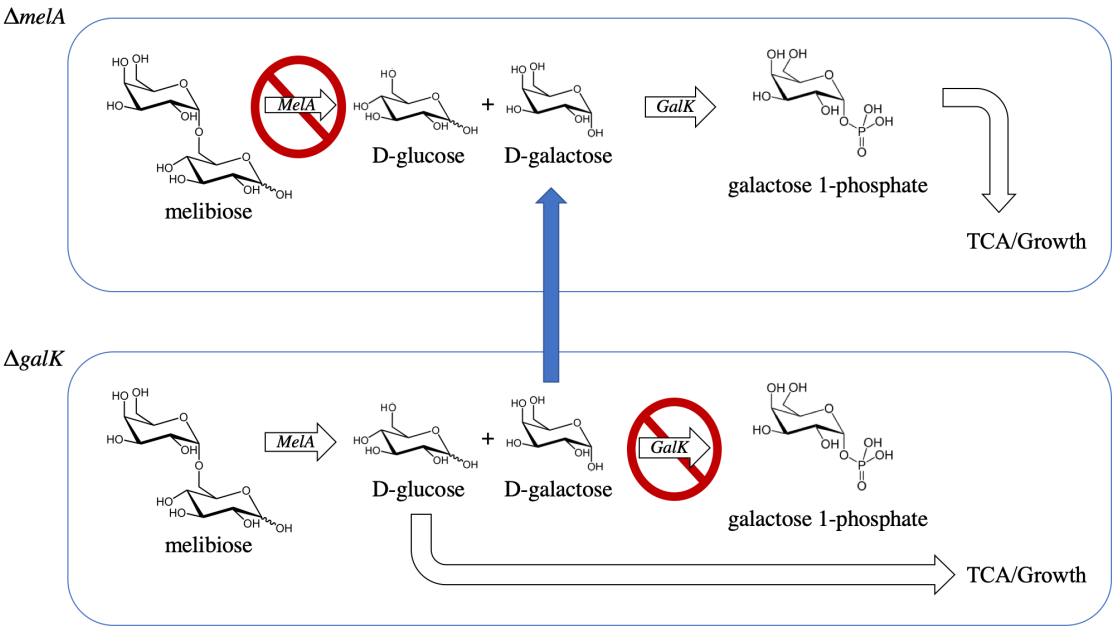

Figure 1: *Proposed Community Metabolism* The diagram depicts the deficiencies of the two cells and how the two might complement one another to form a complete glycolytic pathway for Δ*melA*

When grown on melibiose jointly, we hypothesized the mutants would have a commensalistic relationship: ΔgalK is able to grow on melibiose partially with a functional α-galactosidase but cannot use the D-Galactose product, and ΔmelA can degrade D-Galactose with a functional galactose kinase. The proposed relationship is dependent on the migration of D-Galactose from ΔgalK to ΔmelA. While the metabolite exchange is possible from ΔgalK to ΔmelA, we expect the relationship to be one sided as downstream metabolites of galactose kinase are phosphorylated and unable to cross back and support ΔgalK. We predicted that the commensalism would allow ΔmelA to recover parent phenotype on melibiose, and ΔgalK would remain unchanged if not hindered by the growing ΔmelA. Furthermore, this cyclic, negative feedback towards ΔgalK from ΔmelA, will ultimately stabilize ΔmelA growth which also depends on ΔgalK. To investigate our hypothesis we conducted growth curve experiments with the parent strain and each mutant alone as well as both mutants in the joint culture partitioned by a 3.5 MW-cutoff, dialysis slide-a-lyzer (Thermofisher). Through analysis of the growth of the combined

mutants we were able to elucidate the power of cross-species metabolic interactions on microbial communities.

0.3 Materials and Methods

In order to investigate the potential of co-metabolism we tracked growth cultures of both mutants, the wild-type strain, and the combined culture.

Each of the four cultures was grown in 150mL of MOPS minimal medium (supplemented with 20mM NH4Cl2) [17] in a 250 mL beaker. All cultures contained 0.025% glucose as well as 0.075% melibiose. Cultures were grown shaking in 37C water baths for the duration of the experiment. All cultures were inoculated at an optical density (OD) of 0.05 three hours prior to growth curve sampling and cocultures received an interior inoculation of 0.5 OD (Figure 2). OD was discerned with a Spectronic 20 (Bausch and Lomb) which has a linear range between 0.2 and 0.5 OD for 600 nm light, and thus, higher density samples were diluted with saline 1:1 or 1:3 before measurement.

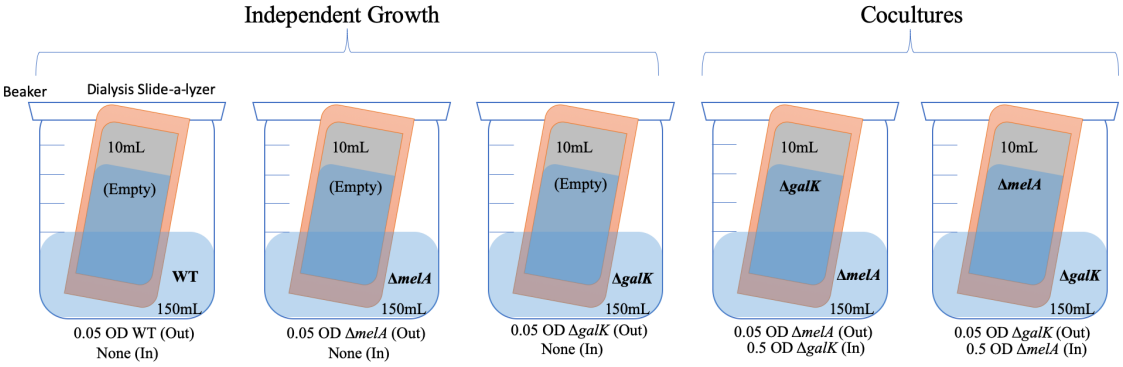

Figure 2: *Experimental Set-Up* The five cultures set up for growth curve measurements. Three independent strain cultures were incoluated outside the dialysis chamber with 0.05 OD and then two cocultures were incoluated similarly but accompanied with interior inoculations of 0.5 OD

During the growth curve sampling, culture fractions were taken for OD at 40 minute and 20 minute intervals in order to capture the diauxotrophic curve in high resolution while minimizing the entire volume disposed. Sample culture was discarded after use. However, the method did not suffice for our cultures originally.

The first cultures was inoculated with one strain each, WT, Δ*melA* or Δ*galK* (see Table 1) and contained empty dialysis containers for standard growth control curves. The third anf fourth cultures contained a dialysis bag (filled with same medium) inoculated with

one of the mutants inoculated at 0.15 surrounded by medium inoculated with the other mutant at 0.05 OD. OD Samples were taken from the outer culture only throughout the experiment.

Strain	**Genotype**	**Description**
BW25113	Parent strain (WT)	F-, DE(araD-araB)567, lacZ4787(del)::rrnB-3, LAM-, rph-1, DE(rhaD-rhaB)568, hsdR514
BW25113 Δ*melA*	Δ*melA*	α-galactosidase (KEGG ec 3.2.1.22)
BW25113 Δ*galK*	Δ*galK*	galactokinase (KEGG ec 2.7.1.6)

Table 1: *Strain Table.* Strains used throughout the experiments of this work[12]

Four Gen III (Biolog) assays, one for WT, one for Δ*melA*, one for Δ*galK* and for the combined Δ*melA* and Δ*galK*, were completed according to the online manual protocol for Protocol A with inoculating fluid IF. OD's of the three strains was standardized to 0.01-0.02 before depositing into the wells, and the combined culture was made by using half volume for each of the two mutants. The Biolog plates were left sitting in a 30C room for 1 week until they were photographed.

The purple intensity of each well was extracted from the photographs using a combination of my own MATLAB (MathWorks) program and script, and one free-to-publish function [23]. The script crops, perspective-corrects, and segments a photo of the underside of a plate and then uses the MATLAB image analysis function 'imfindcircles()' to identify the wells and finally averages the color in the well to take a reading. Note, all colors are converted from sRGB to CIE L*a*b* because sRGB is a poor system for applying distance metrics, and thus poorly sorts and scores comparative photos [18]. Both the code and a visual validation of the program can be found in the Supplemental Information.

0.4 Results and Discussion

0.4.1 Results

In order to investigate the hypothesis, that Δ*galK* would boost the growth of Δ*melA*, we set up five growth experiments with WT *E. coli*, Δ*galK*, Δ*melA*, and the two combinations of the mutants (one in the dialysis box and the other outside) (Figure 2).

First, one must note that our experiments originally yielded confounding results. All four strains remained static (not death, +0.025 OD) within the four hour window. Af-

ter reviewing our previous setup, we concluded that missing any of the other essential ingredients would either result in death or non-static growth, and thus, the mutants had insufficient carbon source. We then dosed in the original amount of melibiose again, 0.075%, and left the experiments to grow overnight (approximately 18 hours).

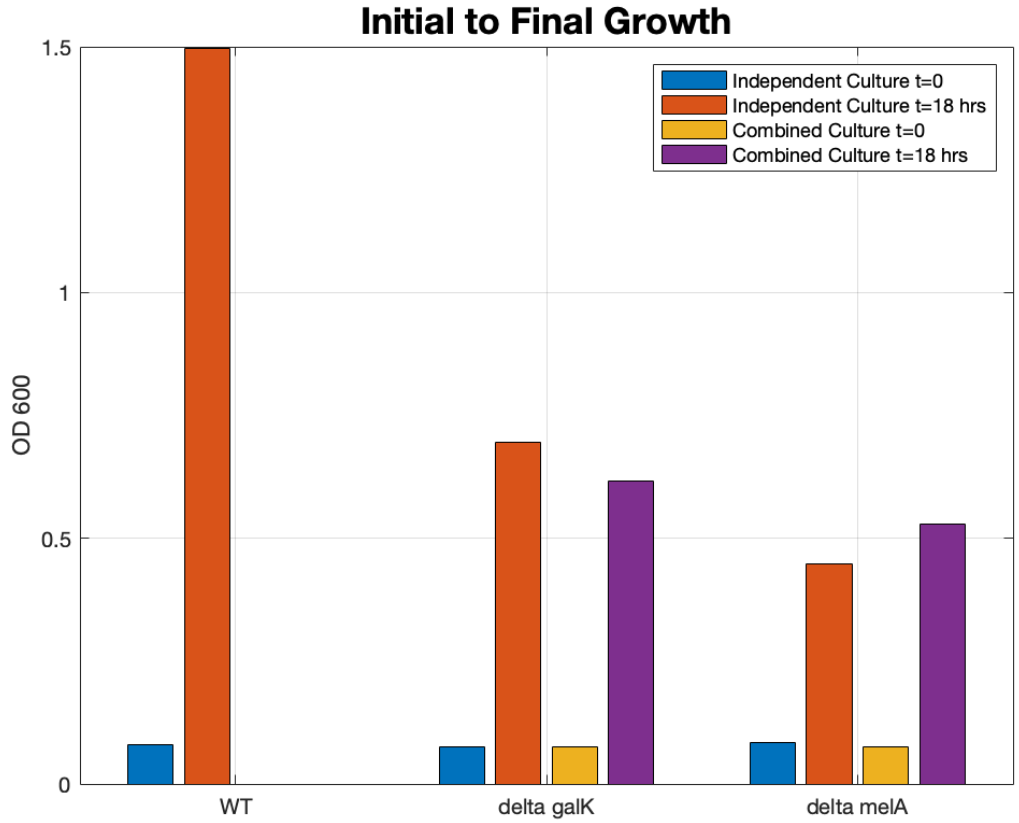

Figure 3: Initial and Final Growth After 18 Hours. *Note the 'Combined Culture' for ΔgalK signifies the culture where ΔmelA was inside the dialysis chamber and ΔgalK in free surrounding medium*

After 18 hours, our WT *E. coli* control culture grew to an OD of 1.496 (Figure 3). This was expected, and confirmed our suspicions that the medium was missing sufficient carbon source for the organism. Additionally, this demonstrated that WT is not impeded by the presence of the empty dialysis box. We assume, that the deficiencies of the mutants would not cause them to be significantly more sensitive than the WT (because of the nature of the deletions) and that any lack of growth is a consequence of their impaired ability to degrade the carbon source.

After 18 hours, the control cultures of independent Δ*galK* and independent Δ*melA*

grew to OD's of 0.696 and 0.448 respectively. This result generally matches our expectations, but highlights some subtle nuances of our mutants. We inferred from the genetics that Δ*galK*' ability to refine melibiose into glucose (Figure 1) would allow it grow substantially (despite its inability to process galactose); if we assume that glucose and galactose contribute to biomass equally, this is almost perfectly described by the Δ*galK* growth which is approximately half that of WT (which can utilize both products of melibiose degradation). On the other hand, Δ*melA* growth is unexpected [15]. While we intended to dose a small concentration of glucose (0.025%), the lack of growth during the four hour window suggests it did not have any effect on final OD, and that the 0.448 was entirely from utilizing melibiose as a carbon source. Previously, the microbial erosion of regenerated cellulose membranes has been demonstrated [19] but poorly characterized; our future experiments will include negative controls. The growth of Δ*melA* on melibiose suggests that the organism has promiscuous carbohydrate enzymes for the catabolism of the sugar which allow it to utilize the sugar. This result is important because if the organism is able to utilize the carbohydrate, the commensalistic relationship will be less important for its growth when the two mutants are combined.

After 18 hours, the two combined cultures, Δ*galK* outside-Δ*melA* in dialyzer and Δ*melA* outside-Δ*galK* in dialyzer, yield growths of 0.616 and 0.528 OD's respectively, where the OD is sampled from the solution outside the box and represents the growth of the mutant outside the dialyzer box. When compared with the independent growth experiments the results of the joint cultures demonstrate the impediment of Δ*galK*'s growth in the presence of Δ*melA*, and alternatively, the augmentation of Δ*melA* growth in the presence of Δ*galK* (In future work, we plan to replicate our experiments to attempt to confirm the significance of the small change in populations). If real, the relationship is less amiable then commensalism and is more like a mild parasitism. As hypothesized, the interaction between the organisms is beneficial for Δ*melA*, allowing the population to obtain more carbon then was available previously but detrimental for Δ*galK* which must compete for melibiose (control culture demonstrates Δ*melA* can use it as a sole carbon source) as well salts, nitrate, phosphate and other resources. Unfortunately, the carbon debacle hinders our view of temporal community dynamics, but from final data, we may hypothesize that community starts with a higher proportion of Δ*galK* to Δ*melA* which gradually lowers as Δ*galK* produces galactose for Δ*melA* and increases its cooperation.

The Biolog assays provide a broader view of the changes in metabolism (Figure 4). The image-analysis script described in the Methods section yields a quantitative perspective of the varying growth of the independent mutants as well as the two combined. The heat

map colors correspond to the difference in WT and mutant strain experiments given by the Euclidean norm of the two colors. All the differences have been normalized by the 95%-confidence interval (4x standard deviation since the difference compares two single points, not a mean and a point) of the variance of all four positive control wells; all values are in absolute units, and those with $|value| < 1$ are not statistically significant. Note, the data are multiplied by negative one from CIE-L*a*b* space so that the more negative/blue values correspond to lighter wells, while the more positive/red regions correspond to darker wells.

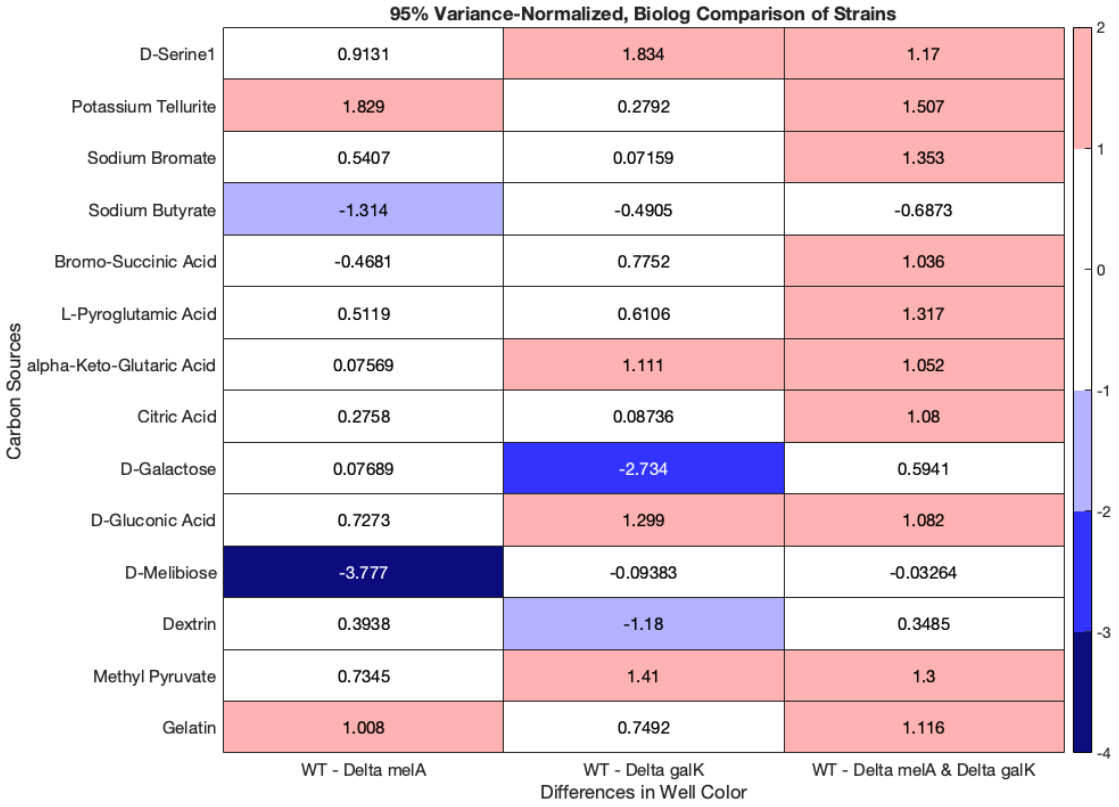

Figure 4: Significant WT-Mutant Differences in Biolog Assay. *Each row corresponds to the (95% confidence) variance-normalized difference in the magnitude of the color in CIE L*a*b* space (produced by the image-acquisition script). Red corresponds to darker well color while blue corresponds to the lighter. The data were extracted from the full set of Biolog experiments (found in the supplemental section) given that one of the three differences had a statistically significant variation from WT* ($|value| > 1$).

The displayed points are a subset of all the Biolog assay data which had at least one statistically significant difference amongst the three comparisons. Of the 14 experiments,

D-melibiose and D-galactose are the strongest and confirm the genetics of the mutants. The majority of the significant differences for the cocultured mutants can be attributed by similar value to one of the adjacent differences between an independent mutant and WT and could be attributed to dominating growth of one of the mutants, however, there are four experiments, Sodium Bromate, Bromo-Succinic Acid, L-Pyoglutamic Acid and Citric Acid, which have significant values that are not recapitulated in the independent mutant cultures suggesting a unique happening. We argue that this is demonstration of the existence of the two species in coculture not only because the unique phenotype "fingerprint" but particularly because of the presence of Sodium Bromate on this list.

When paired with a carbon source, Sodium Bromate is used as a tool for positively selecting mutants incapable of producing acid from sugars by fermentation [20]; it efficiently selects for sugar uptake, glycolytic pathway and excretion mutants which are otherwise elusive [20]. The combination of the mutants having significantly more growth than WT and either of the independent mutants suggests that the combined mutants make less acid than either independently. If the combined well is darker (ie living) then the most likely solution is that they are not fermenting, but rather are complementing each other to form a glycolytic pathway that the WT did not depend on or prefer. This result is important for confirming the potentiality of the proposed intracellular pathway and supports the argument that metabolites are trafficking the community despite that it results in small changes in relative population.

Additionally, the three other unique phenotypes are valuable for understanding the coculture. All of these experiments resulted in net-positive differences compared to WT indicating that the coculture conferred a fitness advantage. While these are more difficult to explain and require further biochemical assays, they are all examples of synergistic fitness of the cocultured mutants and suggest that there are multiple benefits to encourage the interaction of the mutants.

In summary, the Biolog results suggest that the small changes in relative populations are likely to be the influence of the combined communities. While our lack of replicates and small changes in populations encourage us to redo the experiments in the future, the multifaceted data allows us to to understand that we have constructed a community of interacting members. This finding, which mimics our hypothesis and prediction that the co-culture of the two organisms results in supported growth of $\Delta melA$, but also demonstrated the unpredicted, minor inhibition of $\Delta galK$, allows us to consider the effects of the microbial interaction on influencing the community.

0.4.2 Discussion

While the changes in biomass corresponds to approximately -11% and $+15\%$ for $\Delta galK$ and $\Delta melA$, all changes in population can be attributed to the passaging of one metabolite. True communities are composed of thousands of these interactions and can have bidirectional passaging. We may understand that our interaction is indirectly bidirectional, because the growth of $\Delta melA$ involves the consumption of shared resources. However, the data demonstrate that this type of interaction might be valuable for establishing a community as it stabilizes the existence of both members by applying enough evolutionary pressure to persist itself (but potentially not enough to encourage the strains to evolve), which we see in the compromising populations of the two strains in the combined culture.

The community would be nuanced though, one might expect contact between $\Delta galK$ and $\Delta melA$ to lead to the trade of genetic material to supplant respective deficiencies. The frequency of genetic trade is high in thriving microbial communities [Gore] and in such this two member motif would likely collapse. All things considered, physical barriers are abundant in nature and our experimented scenario might mimic the early stages of an intraspecies parasitism, if the mutants were to diverge independently. When partitioned, the $\Delta melA$ gets a small boost for outperforming its competitors and $\Delta galK$ experiences a minor set back but potentially not enough to stress the organism into a gain of function glycolytic pathway (depends on the promiscuity of its carbohydrate degrading arsenal). Our future experiments will test this hypothesis by including the same experiments passaged thousands of generations [21] to test the long term stability of the relationship and potentially observe conception/decay of stronger communal relationships. The research will be valuable as it might allow posterity to test methods for interfering with developing community interactions.

0.5 Conclusion

Our synthetic, two-member *Escheria coli* consortium demonstrates the viability of metabolite interactions for establishing microbial communities. While the growth cultures alone describe small relative changes in population, the Biolog assays reveal the validity of the fluctuations as the coculture of the two mutants has a beneficial, unique phenotypic signature. Particularly the coculture outperforms either mutant independently on Sodium Bromate demonstrating that they are completing a non-fermentive glycolytic pathway like the theoretical cross-catabolism proposed. With this understanding, we can interpret the

combined growth cultures as microbial communities with altered populations due to the presence of the other member: a mildly parasitic interaction exists such that $\Delta melA$ confers a 10% fitness advantage at the cost of 15% the growth of $\Delta galK$. This community serves as a model for how physically separated mutants within a strain population might develop into different species with specific niches.

0.6 Supplemental Information

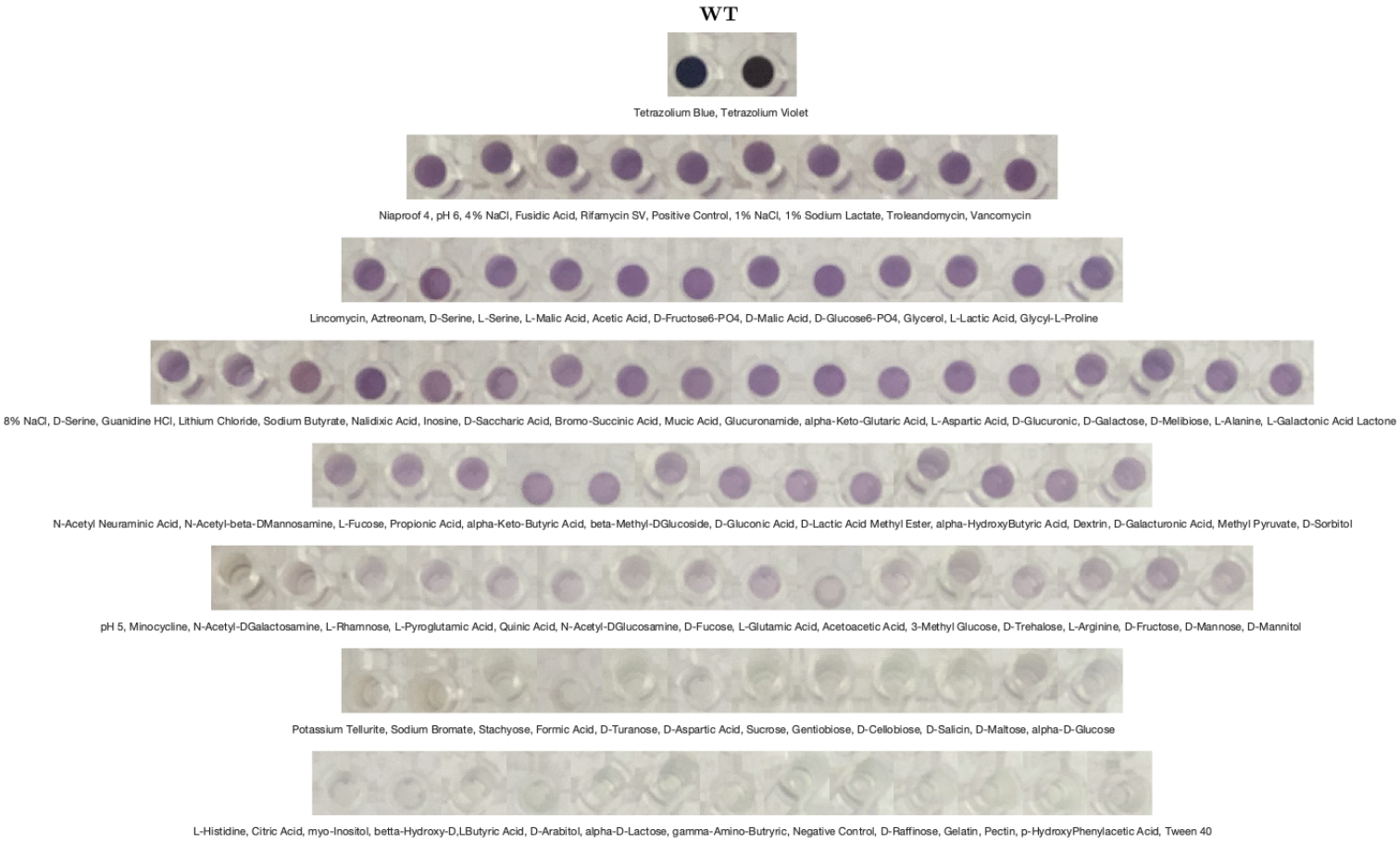

Figure 5: *Visual Validation of Image-Analysis Color Scoring Program* The images of wells are sorted based on their color values extracted by the image analysis program

The code for the Image Analysis program can be found at Will Sharpless' C112 GitHub respository `https://github.com/willsharpless/C112`. The image analysis function is

dubbed 'BiologPlateReader.m' and the script on which I ran mine is 'biolog_histo.m'. If supplied with a photo of the underside of a plate as well as the auxiliary .m files linked in the 'Perspective Correction' section, the code will run with MATLAB 2019a on any cpu (note, the photos used are included in the git repository).

The code is generally validated by 'kmeans' clustering [22] of the color (in CIE L*a*b*) by darkness to see if the arbitrary clusters truly are sorted such that all colors in one cluster match(Figure 5). Note, pH5 is an unuseable experiment as it clusters improperly because of minimal pink light coming through my hand in the image influences the darkness of the well. Note, also that the

The entire heatmap of all Biolog experiments can be found below (Figure 6). Note, the majority of comparisons are statistically insignificant (white and light red). Also, the values were not flipped (negative values correspond to darker wells) but the colors still match the darkness of the well (blue values correspond to lighter wells).

0.7 Acknowledgements

We would like to thank GSI's Dylan McClung and Sean Carim for their vital criticism that propelled this work to its final state, as well as Professor Matt Traxler for his enthusiastic support of our elaborate scientific endeavors. Thank you guys this project was very interesting and a lot more fun than characterizing lactose diauxotrophs!

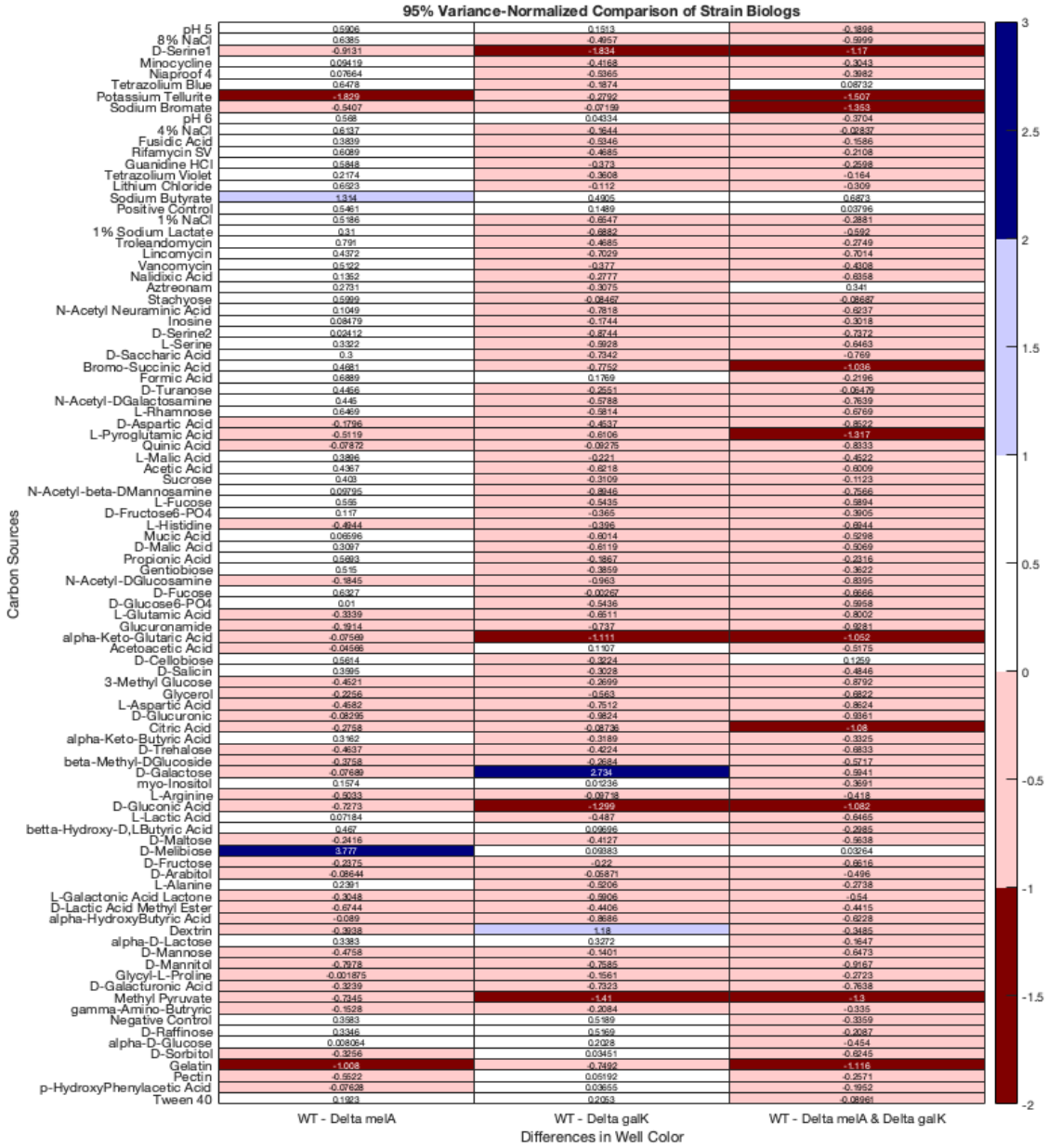

Figure 6: *All Biolog Experiments* Note the color is slight different from the figure in the Results section such that the white and light red values are both statistically insignificant.

References

1. Friedman J, Gore J. (2017). Ecological systems biology: The dynamics of interacting populations. Curr Opin Syst Biol 1:114–121

2. Venturelli OS, Carr AV, Fisher G, Hsu RH, Lau R, Bowen BP, Hromada S, Norther T, Arkin AP. (2018). "Deciphering Microbial Interactions in Synthetic Human Gut Microbiome Communities." Molecular Systems Biology, vol. 14, no. 6, 2018

3. Hastings A, Harrison S. (1994). "Metapopulation Dynamics and Genetics". Annual Review of Ecology and Systematics. 25 (1): 167–188.

4. Arevalo P, Vanlnsberghe D, Elsherbini J, Gore J, Polz MF. (2019). "A Reverse Ecology Approach Based on a Biological Definition of Microbial Populations." Cell, vol. 178, no. 4, 2019

5. Kuypers, MM, Marchant HK, Kartal B. (2018). The microbial nitrogen-cycling network. Nat. Rev. Microbiol. 16, 263–276

6. Coyte, KZ, Schluter J, Foster KR. (2015). "The Ecology of the Microbiome: Networks, Competition, and Stability." Science, vol. 350, no. 6261, May 2015, pp. 663–666

7. Gurav R, Lyu HH, Ma JL, Tang JC, Liu QL, and Zhang HR. (2017). Degradation of n-alkanes and PAHs from the heavy crude oil using salt-tolerant bacterial consortia and analysis of their catabolic genes. Environ. Sci. Pollut. Res. 24, 11392–11403

8. Lakshmanan V, Ray P, Craven KD. (2017) Toward a Resilient, Functional Microbiome: Drought Tolerance-Alleviating Microbes for Sustainable Agriculture. In: Sunkar R. (eds) Plant Stress Tolerance. Methods in Molecular Biology, vol 1631. Humana Press, New York, NY

9. Rosenbaum M, Knight R, Rudolph L. (2015). "The Gut Microbiota in Human Energy Homeostasis and Obesity." Trends in Endocrinology and Metabolism, vol. 26, no. 9, 2015, pp. 493–501

10. Lyte M. (2014) Microbial Endocrinology and the Microbiota-Gut-Brain Axis. In: Lyte M., Cryan J. (eds) Microbial Endocrinology: The Microbiota-Gut-Brain Axis in Health and Disease. Advances in Experimental Medicine and Biology, vol 817. Springer, New York, NY

11. Johnson, Katerina VA, Foster KR. (2018). "Why Does the Microbiome Affect Behaviour?" Nature Reviews Microbiology, vol. 16, no. 10, 2018, pp. 647–655

12. Baba T, Ara T, Hasegawa M, Takai Y, Okumura Y, Baba M, Datsenko KA, Tomita M, Wanner BL Mori H. (2006). Construction of *Escherichia coli* K-12 in-frame, single-gene knockout mutants: the Keio collection. Molecular Systems Biology, 2, 2006.0008

13. Keseler IM, Mackie A, Santos-Zavaleta A, Billington R, Bonavides-Martinez C, Caspi R, Fulcher C, Gama-Castro S, Kothari A, Krummenacker M, Latendresse M, Muniz-Rascado L, Ong Q, Paley S, Perlata-Gil M, Subhraveti P, Velazque-Ramirez D, Weaver D, Callado-Vides J, Paulsen I, Karp PD. (2017). "EcoCyc: reflecting new knowledge about Escherichia coli K-12", Nucleic Acids Research 45:D543-50

14. Suzuki H, Li SC, Li YT. (1970). Alpha-galactosidase from *Mortierella vinacea*. Crystallization and properties. The Journal of biological chemistry. 1970;245(4):781–6

15. Schmitt R, Rotman B. (1966). alpha-Galactosidase activity in cell-free extracts of *Escherichia coli*. Biochemical and Biophysical Research Communications, 22(5), 473-479

16. Kurahashi, K. 1957. Enzyme formation in galactose-negative mutants of *Escherichia coli*. Science 125:114–116

17. Neidhardt FC, Bloch PL, Smith DF (1974). Culture medium for *Enterobacteria*. J Bacteriol 119(3): 736-747

18. Zeileis A, Hornik K, Murrell P. (2009). "Escaping RGBland: Selecting Colors for Statistical Graphics" (PDF). Computational Statistics & Data Analysis. 53: 3259–3270.

19. Weng R, Chen L, Lin S, Zhang H, Wu H, Liu K, Huang L. (2017). Preparation and Characterization of Antibacterial Cellulose/Chitosan Nanofiltration Membranes. Polymers, 9(4), 116

20. Winkelman JW, Clark DP. (1984). Proton suicide: general method for direct selection of sugar transport and fermentation-defective mutantsJ. Bacteriol. , 160, 687–690.

21. Lenski, RE, Travisano M. (1994). Dynamics of adaptation and diversification: a 10,000-generation experiment with bacterial populations. Proceedings of the National Academy of Sciences, USA 91:6808-6814.

22. Lloyd, SP. (1982), "Least squares quantization in PCM" (PDF), IEEE Transactions on Information Theory, 28 (2): 129–137, doi:10.1109/TIT.1982.1056489.

23. Chan, M. (2012). "Perspective-Control-Correction". Mathworks. Retrieved from https://www.mathworks.com/matlabcentral/fileexchange/35531-perspective-control-correction.